

Figure 1. Two-dimensional geometrical description: heart domain Ω_H , torso domain Ω_T (extramyocardial regions), heart-torso interface Σ and torso external boundary Γ_{ext} .

conditions of the monodomain problem. The precise definitions of \mathbf{g} and I_{ion} depend on the electrophysiological transmembrane ionic model. In the present work we make use of one of the human myocyte model Beeler Reuter [5]. Ω_H stands for the heart domain which is in our case the atria. In order to simulate the body surface potential we first need to compute the extracellular potential in the heart. Supposing the the extracellular conductivity tensor $\sigma_e = \lambda \sigma_i$, where σ_i is the intracellular conductivity tensor and $\lambda \in \mathbb{R}$. The extracellular potential satisfies

$$(\lambda + 1) \operatorname{div}(\sigma_i \nabla u_e) = - \operatorname{div}(\sigma_i \nabla v_m). \quad (2)$$

One can easily check that

$$u_e = \frac{1}{(1 + \lambda)} (\langle v_m \rangle - v_m) \quad (3)$$

is a solution of equation (2). Moreover, it is the unique solution satisfying $\left(\int_{\Omega_H} u_e \right) = 0$.

Here, $\langle v_m \rangle = \frac{1}{|\Omega_H|} \int_{\Omega_H} v_m$ is the mean value of v_m in space. In order to compute the body surface potential we need to solve a Laplace equation on the torso with a Dirichlet boundary condition on the heart-torso interface [4].

$$\begin{cases} \operatorname{div}(\sigma_T \nabla u_T) = 0, & \text{in } \Omega_T, \\ \sigma_T \nabla u_T \cdot \mathbf{n} = 0, & \text{on } \Gamma_{ext}, \\ u_T = u_e, & \text{on } \Sigma. \end{cases} \quad (4)$$

The forward problem algorithm is: (a) compute the transmembrane potential by solving equation (1), (b) compute the extracellular potential using the formula (3), (c) compute the torso potential by solving (4). As it was explained in the introduction we build a synthetic data base of BSPs and their correspondant EGMs. Each sample of BSPs and EGMs corresponds to a stimulation location. We simulated n heart beats, each one corresponds to a given I_{stim} . We use finite element method in order to solve equations (1) and (4), a space discretisation of the heart and torso domains is then needed. Since we are interested in targeting ectopic beats in the atria, we only consider the electrical activation in the atria. The finite element geometry of atria is given in Figure 2.1 (left). it was embedded in a torso geometry given in Figure 2.1 (right) [6].

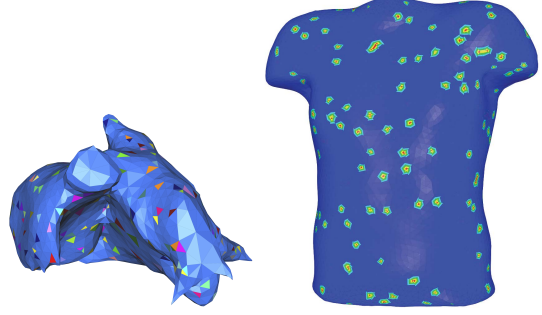


Figure 2. Finite element computational domains: Atria geometry with the different locations of stimulus used to construct the training data set (lfet). Torso geometry with different BSP measurements locations (right).

2.2. Inverse problem: a regression method

As explained in the previous paragraph, we have n samples of BSP and EGMs. The sequence $(BSP_i, EGM_i)_{i=1 \dots n} \in \mathbb{R}^{p \times m} \times \mathbb{R}^{q \times m}$ is the data set of our metamodel. Here p (respectively, q) is the number of potential measurement locations on the body surface (respectively, on the heart surface), and m is the number of time steps. We denote by $(x_k)_{k=1 \dots p}$ (respectively, $(y_k)_{k=1 \dots q}$) the positions of the BSP measurements (respectively, positions of EGMs measurements) and $(t_l)_{l=0 \dots m-1}$ the times of the recordings. For the i^{th} element of our data set we have, $BSP_i \in \mathbb{R}^{p \times m}$, where $BSP_i(l \times p + k) = u_T(x_k, t_l)$, for $k = 1, \dots, p$ and $l = 0, \dots, m-1$, and $EGM_i \in \mathbb{R}^{q \times m}$ where, $EGM_i(l \times q + k) = u_e(y_k, t_l)$, for $k = 1, \dots, q$ and $l = 0, \dots, m-1$.

The main goal is to build a function f able to accurately map a BSP to an EGM. We use a kernel ridge regression method based on the gaussian kernel

$$K(\mathbf{x}, \mathbf{y}) = e^{-\frac{|\mathbf{x} - \mathbf{y}|^2}{2\sigma^2}}, \quad \forall \mathbf{x}, \mathbf{y} \in \mathbb{R}^{m \times p}.$$

We look for f in a *Reproducing Kernel Hilbert Space* (RKHS) $(\mathcal{H}, \langle \cdot, \cdot \rangle_{\mathcal{H}})$ characterized by the following property,

$$\forall f \in \mathcal{H}, \quad \forall \mathbf{x} \in \mathbb{R}^{m \times p}, \quad f(\mathbf{x}) = \langle \mathbf{f}(\cdot), \mathbf{K}(\cdot, \mathbf{x}) \rangle_{\mathcal{H}}. \quad (5)$$

where $\langle \cdot, \cdot \rangle_{\mathcal{H}}$ is the inner product in \mathcal{H} . The use of the Gaussian kernel can be motivated by the following property (see [7]): given a compact subset K of $\mathbb{R}^{m \times p}$, the set of the restriction to K of functions from \mathcal{H} is dense in the set of continuous functions from K to \mathbb{R} . In other word, \mathcal{H} is rich enough to approximate any possible continuous mapping from the BSP to a given lead of the EGM.

Consider in \mathcal{H} the following regularized least square problem: given a training set $\{(\mathbf{x}_i, \mathbf{y}_i)\}_{i=1}^n \in (\mathbb{R}^{m \times p} \times$

$\mathbb{R})^n$, solve

$$\min_{f \in \mathcal{H}} \left\{ \frac{1}{n} \sum_{i=1}^n (f(\mathbf{x}_i) - \mathbf{y}_i)^2 + \lambda \|f\|_{\mathcal{H}}^2 \right\}, \quad (6)$$

where $\lambda > 0$ is a given regularization coefficient and n is the number of the data set element. The representer theorem ([6]) states that the solution to (6) can be written as:

$$\sum_{i=1}^n \alpha_i K(\cdot, \mathbf{x}_i),$$

where $\alpha = (\alpha_i)_{i=1 \dots n} \in \mathbb{R}^n$ is the new unknown. Defining the Gram matrix $K = (K_{ij})_{i,j=1 \dots n}$ with $K_{ij} = K(\mathbf{x}_i, \mathbf{x}_j)$, the training problem (6) is equivalent to solving:

$$\min_{\alpha \in \mathbb{R}^n} \left\{ \frac{1}{n} (K\alpha - \mathbf{y})^T (K\alpha - \mathbf{y}) + \lambda \alpha^T K \alpha \right\},$$

whose solution is given by

$$\alpha = (K + \lambda n I)^{-1} \mathbf{y}. \quad (7)$$

Here $\mathbf{y} \in \mathbb{R}^n$, and the i^{th} element of \mathbf{y} represents an element of EGM_i meaning the value of u_e in a fixed position at a given time. In order to consider all the positions on the atria surface and all the time sequence. The training phase consists in solving this system:

$$A = (K + \lambda n I)^{-1} Y, \quad (8)$$

with $A, Y \in \mathbb{R}^{n \times (q \times m)}$, where $Y = (EGM_i^T)_{i=1 \dots n}$. Once the training phase is completed, the reconstruction of EGM from a given heart beat $BSP \in \mathbb{R}^{p \times m}$ is obtained, according to (5), by

$$EGM = \tilde{K} A, \quad (9)$$

with $\tilde{K}_i = K(BSP, BSP_i), i = 1 \dots n$.

3. Results

In this section we present numerical simulations of the forward and inverse problems. We first built $n = 400$ heart beats using our computer simulator as described in section (2.1). In this work we reconstruct the EGMs on all the whole atria surface ($q = 1994$), from 264 BSPs ($p = 264$). In figure 3 we present two example of simulation depending on the location of the stimulus, in each case we show two snapshots one at 10ms (left) and the other at 90 ms (right). In the top two figures we show an example of simulation where the atria is activated in the left superior pulmonary vein and in figure 3 (bottom) the right atria appendage is activated. After building the meta-

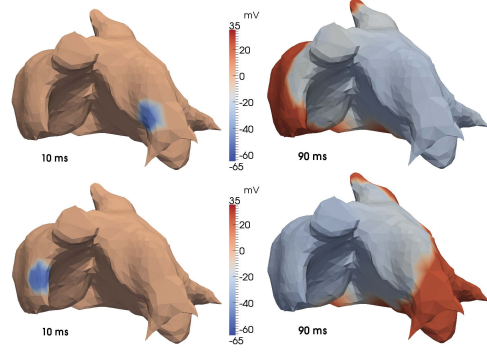


Figure 3. Snapshots of the simulated extracellular potential. The atria is activated in the pulmonary vein (top) and in the right atria (bottom).

model from equation (8), we propose to test the regression method on different example. As expected the reconstruction of EGMs from BSPs belonging to the training data set is perfectly accurate. On the contrary, if the BSP does not belong to the training data set, the accuracy of the EGMs reconstruction is not accurate especially in terms of amplitude where the l^∞ relative error could reach 50%, an example is given in figure 4 where the amplitude of the exact solution (continuous red line) is twice higher then the RKHS solution (dashed green line). Nevertheless, the

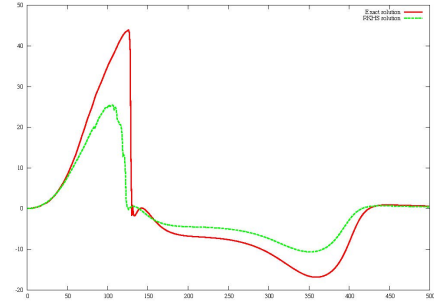


Figure 4. Comparison between the exact and the reconstructed EGM at a given location on the atria: Exact solution (red continuous line) and the one reconstructed with RKHS (green dashed line).

reconstructed and original signals are synchronized. We then computed the activation times following the maximum time derivative of the extracellular potential at each node of the mesh. The maximal error is 6ms. The location of the stimulus corresponds to the location of the minimal activation time. For the sake of illustration we show in figure 4 a comparison of the activation times computed from the original signal (left) and the reconstructed (right). The activation site is localized with a 0.5 cm of accuracy, which is expected since the average of the distance between the stimulus sites in the training set is 0.42 cm.

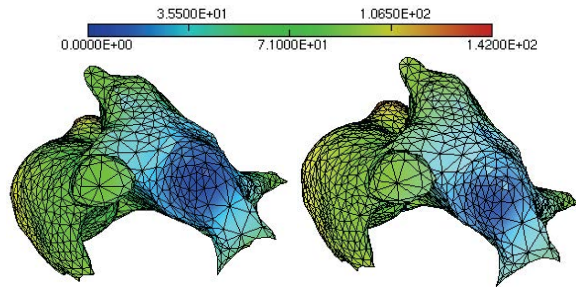


Figure 5. Comparison of the activation times: exact activation times (left) and activation times reconstructed with RKHS metamodel (right).

4. Discussion

In this work we showed an original approach based on a machine learning technique in order to solve the inverse problem in electrocardiography. This method allows solving the inverse problem in real time: since the metamodel could be build off-line, in practice we only need to evaluate the metamodel according to equation (9). This does not require solving any linear system. The reconstruction of EGMs is accurate if the training data base is sufficiently rich. The accuracy of the produced EGMs depends on how close is the BSP from the elements of the training set. This means that it is difficult to reproduce an information which is far from the training data base. It is for instance difficult to reproduce accurate EGM for a multiple sites activation based on a data set containing only simulation with single site stimulus. This limitation could be tackled by including multiple site stimulations in the training data set, at the same time this will increase the complexity of the training phase. But since this phase is off line, the computational time of the reconstruction would be slightly affected.

5. Conclusion

In this work we have considered a machine learning approach, based on the kernel ridge regression method, in order to construct activation maps on the atria from a set of BSP measurements. The procedure has been trained using synthetic data from numerical simulations, based on a 3D mathematical model of the ECG involving a mathematical description of the electrical activity of the heart and the torso. Several examples showed the method is able to reconstruct conveniently the EGM information included in the training data set, and is robust when reconstructing situations close to the training data set. In this study we showed that a single site stimulus is localized with 0.5 cm error. The accuracy could be improved if the training set is much rich. In the proposed approach, the solution depends on all training examples, which may be too expensive. This point could be improved in future works. In

future works this method would be trained and tested on clinical data. The ECG simulator would be used in order to enrich the clinical data.

Acknowledgements

This work was partially supported by an ANR grant part of Investissements dAvenir program reference ANR-10-IAHU-04

References

- [1] Ghosh S, Rudy Y. Application of l_1 -norm regularization to epicardial potential solution of the inverse electrocardiography problem. *Annals of Biomedical Engineering* 2009; 37(5):902912.
- [2] Scholkopf B, Smola AJ. *Learning with Kernels: Support Vector Machines, Regularization, Optimization, and Beyond*. Adaptive Computation and Machine Learning. Cambridge, MA, USA: MIT Press, 2001.
- [3] Sundnes J, Lines G, Cai X, Nielsen B, Mardal KA, Tveito A. *Computing the electrical activity in the heart*. Springer-Verlag, 2006.
- [4] Boulakia M, Cazeau S, Fernández M, Gerbeau J, Zemzemi N. Mathematical modeling of electrocardiograms: a numerical study. *Annals of biomedical engineering* 2010; 38(3):1071–1097. ISSN 0090-6964.
- [5] Beeler G, Reuter H. Reconstruction of the action potential of ventricular myocardial fibres. *J Physiol Lond* 1977;268:177–210.
- [6] Klepfer R, Johnson C, MacLeod R. The effects of inhomogeneities and anisotropies on electrocardiographic fields:a three-dimensional finite element study. *IEEE Eh4BC and CMBEC* 1995;.
- [7] Saunders C, Gammerman A, Vovk V. Ridge regression learning algorithm in dual variables. In *ICML*. 1998; 515–521.

Address for correspondence:

Nejib Zemzemi
 INRIA Bordeaux Sud-Ouest, 200 rue de la vieille tour, 33405
 Talence France.
 nejib.zemzemi@inria.fr